

Electromagnetic response of anisotropic eutectic metamaterials in THz range

A. Reyes-Coronado¹, M. F. Acosta³, R. I. Merino³, V. M. Orera³, G. Kenanakis¹,
N. Katsarakis^{1,4}, M. Kafesaki^{1,2} and C. M. Soukoulis^{1,2,5}

¹*Institute of Electronic Structure and Laser (IESL), Foundation for Research and Technology Hellas (FORTH),
P.O. Box 1385, 71110 Heraklion, Crete, Greece*

²*Department of Materials Science and Technology, University of Crete, 71003 Heraklion, Greece*

³*Instituto de Ciencia de Materiales de Aragón, CSIC-Universidad de Zaragoza, E-50018 Zaragoza, Spain*

⁴*Science Department, Technological Educational Institute of Crete, 71004 Heraklion, Crete, Greece*

⁵*Ames Laboratory-USDOE, and Department of Physics and Astronomy, Iowa State University, Ames, Iowa 50011,
USA*

Abstract. We study the electromagnetic response of anisotropic eutectic metamaterials, consisting in cylindrical polaritonic LiF rods embedded in a KCl host. The reflectance of samples was obtained by measuring the specular reflectance at far infrared. Modeling the eutectic materials and solving numerically Maxwell equations, we obtained simulated reflection. In addition of simulated and experimental data, we considered the reflectance expected from simple effective response functions models, obtaining a good agreement between all three sets of data. From the effective response functions models, we obtain a range of frequencies in which the system behaves as a homogeneous effective anisotropic media, with a hyperbolic dispersion relation, opening possibilities for negative refraction and focusing.

Keywords: eutectic materials, effective medium, hyperbolic dispersion relation.

PACS: 41.20.Tb, 42.70.Qs, 81.05.Xj, 78.67.Pt

INTRODUCTION

Metamaterials are engineered composites that possess novel electromagnetic properties not observed in their constituent materials. Such materials have attracted attention because of their unusual properties as negative refractive index,^[1-5] giant dielectric constant,⁶ permittivity close to zero⁷, near-field focusing and subwavelength imaging.⁸ Despite the rather rapidly development of the electromagnetic theory and simulation in the metamaterial field, the metamaterial samples are manufactured by difficult and time-consuming methods with limited possibilities, limiting the scope of possible applications. However, one promising way to overlap these limitations is the use of self-organized materials, such as directional solidification eutectics.⁹ Materials obtained through this method present very high anisotropy and can be obtained in large macroscopic pieces.

It has been shown⁸ that a particular anisotropic medium that possess a negative dielectric permittivity component ϵ_{\perp} along the direction perpendicular to the

interface, while the other dielectric permittivity ϵ_{\parallel} remains positive, as well as the magnetic permeability, has a hyperbolic dispersion relation. This means that subwavelength imaging and focusing can occur also in some uniaxially anisotropic media, which can have lower losses and it will be easier to fabricate.

RESULTS AND DISCUSSION

The studied eutectic samples were fabricated using the Bridgman directional solidification technique, which allows growing a well-ordered and long-size dielectric microstructure. The dimensions of the samples are around one square centimeter for their cross sections and several centimeters long, which assure the possibility of characterizing the samples by standard reflection measurement techniques. The eutectic materials consist of cylindrical polaritonic rods made of LiF, embedded in a KCl host, forming a quasi-hexagonal lattice. The diameters and the separations distances between the rods depends on the extraction pulling rate of the material from the furnace (three-zone Hobersal furnace), ranging the diameters

between 0.77 μm and 3.1 μm , while keeping the volume filling fraction constant at $\sim 6.95\%$, that is, with a range in separations distances of 2.8-11.2 μm (see Table 1).

TABLE 1. Diameters and separation distances of rods.

Pulling rate [mm/hr]	Distance between cylinders [μm]	Diameter of cylinders [μm]
4	11.2	3.1
6	8.1	2.6
10	7.8	2.2
100	2.8	0.77

Reflectance from the different eutectic samples was measured at both 13° and 30° angles of incidence using a Bruker IFS 66v/S apparatus in a specular reflectance mode, within the far IR region of the electromagnetic spectrum: 20-100 μm (3-15 THz). The reflectance of both polarizations, parallel and perpendicular to the main axis of cylinders, was measured.

The eutectic samples were simulated using a commercial software (*CST Microwave Studio*), which solves Maxwell equations in both time and frequency domains. For the numerical calculations, we consider the polaritonic rods as perfect cylindrical rods, that is, with circular cross section. However, there is experimental evidence that the cross section of the rods have a hexagonal-type shape with rounded tips. This effect is more evident in the low pulling rate samples, or greater diameters. These deviations in shape will shift moderately the scattering resonances of the rods to higher frequencies, and consequently blue-shifting the reflection peak of the whole system. Since our aim in this paper is to show the feasibility of characterizing an eutectic sample with simple effective medium theories, which possess a range of frequencies where the dispersion relation is hyperbolic, we will not go into much detail at this respect.

The dielectric permittivities for both polaritonic LiF and KCl materials were taken from Palik¹⁰. Polaritonic materials are polar crystals, usually made of two or more different kind of atoms arrange in a lattice, that sustain phonon-polariton resonances due to photon induced optical excitation of transverse phononic modes in the crystal. Polaritonic materials can be modeled using a lorentzian model¹¹ for the dielectric permittivity, given by

$$\epsilon(\omega) = \epsilon_{\infty} - \frac{(\epsilon_0 - \epsilon_{\infty})\omega_{TO}^2}{\omega^2 - \omega_{TO}^2 + i\omega\Gamma}, \quad (1)$$

where $\epsilon_0 = \epsilon(0)$ and $\epsilon_{\infty} = \epsilon(\infty)$ stand for the asymptotic values of the dielectric permittivity at zero and infinity frequencies, respectively. ω_{TO} denotes the transversal optical phonon frequency and Γ stands for the collision

frequency. For LiF, the fitting parameters are $\epsilon_0 = 8.705$, $\epsilon_{\infty} = 2.027$, $\omega_{TO} = 0.038\text{eV}$ and $\Gamma = 0.0022\text{eV}$, while for KCl are $\epsilon_0 = 4.430$, $\epsilon_{\infty} = 2.045$, $\omega_{TO} = 0.017\text{eV}$ and $\Gamma = 0.0065\text{eV}$.

In Fig. 1 we show a representative case from the eutectic samples studied, in which we plot the reflectance obtained experimentally and numerically, for both polarizations.

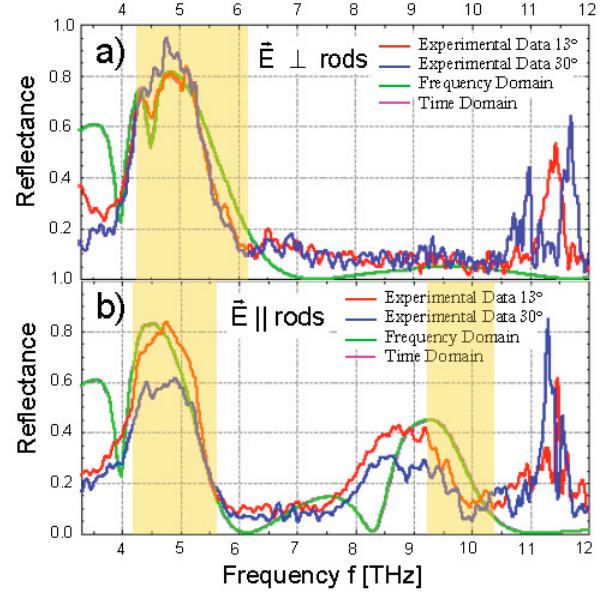


FIGURE 1. (Color online) Reflectance of eutectic LiF cylindrical rods embedded in KCl host sample. Measurements of the reflectance at 13° and 30° angles of incidence (red and blue curve, resp.) and simulated reflectance using frequency and time domain calculations (green and magenta curves, resp.), for both polarizations: a) electric field perpendicular and b) parallel, to the main axis of the cylinders. The vertical yellowish regions correspond to the negative parts of the real part of the effective dielectric permittivity, for both polarizations.

In the upper (lower) part of Fig. 1, we show the reflectance data for a polarization perpendicular (parallel) to the main axis of the cylinders. In red and blue, we plot the experimental reflectance data obtained using 13° and 30° angles of incidence, respectively. We see only one broad peak in the reflectance for the perpendicular polarization (see Fig. 1a), located between 4.3 and 6.2 THz, while we see two main peaks for the parallel polarization (see Fig. 1b), located at 4-5.5 THz and 8-9.5 THz. The experimental features seen between 11 THz and 12 THz correspond to a well-known noise problem from the equipment and contain no physics behind. In Fig. 1 a) and b) we include the numerical calculations for both polarizations, both frequency and time domain calculations (green and magenta curves). In Fig. 1 is hard to distinguish the time domain calculations

because practically both frequency and time domain calculations coincide for all the frequencies considered. This fact was systematically corroborated for all modeled eutectic samples and gives us confidence about the numerical results. We see that for both polarizations we have a very nice agreement between experimental and simulated data. Actually we observe that, for the polarization perpendicular to the cylinders, there are actually two superimposed reflectance peaks located at around 4.4 THz and 4.8 THz, which are well reproduced by the simulations (see in Fig. 1 a), the experimental data taken at 13° angle of incidence).

We consider simple effective medium models for the dielectric effective permittivity of the eutectic samples, for both polarizations: Maxwell-Garnett formula ϵ_{eff}^{MG} for the perpendicular polarization and the so-called simple effective formula ϵ_{eff}^S for parallel polarization. The Maxwell-Garnett formula is given by

$$\epsilon_{eff}^{MG}(\omega) = \epsilon_{host}^{KCl} \frac{(1+f)\epsilon_{Cyl}^{LiF} + (1-f)\epsilon_{host}^{KCl}}{(1-f)\epsilon_{Cyl}^{LiF} + (1+f)\epsilon_{host}^{KCl}}, \quad (2)$$

where ϵ_{Cyl}^{LiF} and ϵ_{host}^{KCl} are the dielectric permittivities of LiF and KCl materials, and f is the volume filling fraction; and the simple effective formula is given by

$$\epsilon_{eff}^S(\omega) = f\epsilon_{Cyl}^{LiF} + (1-f)\epsilon_{host}^{KCl}. \quad (3)$$

Since both the dielectric permittivities of LiF and KCl are complex quantities, the effective medium models give us also a complex quantity for the effective dielectric permittivity. Looking at the real part of the effective dielectric permittivities, specifically to those frequency ranges in which it is negative, we can identify the regions where a high reflectance should appear. These regions are denoted in Fig. 1 as yellowish regions.

We see that, for the perpendicular polarization (see Fig. 1a), we have a nice agreement between the expected position of the reflection peaks from the effective medium models with the experimental and simulated data. For the parallel polarization (see Fig. 1b), we also see a nice agreement for the peak located at low frequencies (centered around 4.6 THz), that we know corresponds to the reflectance from the KCl bulk (by simply looking at the negative part of the real dielectric permittivity). For the second experimentally peak of reflection, located around 9 THz, the expected reflection peak is between 9.2 THz and 10.4 THz, however the effective models do not take into account the geometry of the inclusions. We know that the intrinsic resonances of the cylinders will red-shift the reflected peak and we already explain that in the real

eutectic samples, the rods are not perfectly circular and we have also a dispersion in sizes, that can be responsible for the shift between the simulations and the experimental data.

CONCLUSIONS

We have studied eutectic polaritonic samples, consisting of cylindrical LiF rods embedded in a KCl host. We have measured the reflectance of the samples for both polarizations: perpendicular and parallel to the main axis of the rods, in the THz region. We have compared and obtained good agreement between the experimental data and the numerical calculations performed. We have shown that simple effective dielectric permittivity models can fit the data, and with these models we obtain an anisotropic effective medium, with frequency ranges in which the dispersion relation of the material is hyperbolic, opening the possibility of subwavelength imaging and focusing.

ACKNOWLEDGMENTS

The European Community through the ENSEMBLE project sponsored this work.

REFERENCES

1. V. G. Veselago, USPEKHI 1968, 10, pp. 509.
2. D. R. Smith, W. J. Padilla, D. C. Vier, S. C. Nemat-Nasser, S. Schultz, Phys. Rev. Lett. 2000, 84, pp. 4184.
3. V. M. Shalaev, Nat. Photonics 2007, 1, pp. 41.
4. C. M. Soukoulis, S. Linden, M. Wegener, Science 2007, 315, pp. 47.
5. D. R. Smith, J. B. Pendry, M. C. K. Wiltshire, Science 2004, 305, pp. 708.
6. C. Pecharrromán, Adv. Mater. 2001, 13, pp. 1541.
7. N. Engheta, Science 2007, 317, pp. 1698.
8. A. Fang, T. Koschny, C. M. Soukoulis, Phys. Rev. B 2009, 79, 245127.
9. D. A. Pawlak, S. Turczynski, M. Gajc, K. Kolodziejek, R. Diduszko, K. Rozniatowski, J. Smalc, I. Vendik, Adv. Funct. Mater. 2010, 20, pp. 1116.
10. E. D. Palik, *Handbook of Optical Constants of Solids* (Academic Press Inc., Orlando, 1985).
11. C. Kittel, *Introduction to solid state physics* 8th Ed. (Wiley & Sons, New Caledonia, 2004).